Scientific Research Publishing

Journal of Geoscience and Environment Protection, 2023, 11, 210-220
https://www.scirp.org/journal/gep
ISSN Online: 2327-4344
ISSN Print: 2327-4336

Morphotectonic Analysis along the Eastern Chiang Khong Basin, Chiang Rai, Northern Thailand

Pichawut Manopkawee

Department of Geological Sciences, Faculty of Science, Chiang Mai University, Mueang Chiang Mai, Chiang Mai, Thailand
Email: pichawut.m@cmu.ac.th

How to cite this paper: Manopkawee, P. (2023). Morphotectonic Analysis along the Eastern Chiang Khong Basin, Chiang Rai, Northern Thailand. *Journal of Geoscience and Environment Protection, 11,* 210-220.
https://doi.org/10.4236/gep.2023.114013

Received: April 10, 2023
Accepted: April 27, 2023
Published: April 30, 2023

Abstract

Chiang Khong Basin (CKB) is a northeast-southwest active basin in Chiang Rai province, northern Thailand. The basin is bounded to the east by numerous fault segments of the Mae Ing Fault Zone (MIFZ), where they have triggered several previous earthquakes in Chiang Rai and vicinities. Although the slip of the MIFZ has triggered some earthquakes, the active deformation of the landscape affected by the tectonic processes of the MIFZ is mainly unknown. According to uniform lithologic and climatic conditions across the MIFZ, we rely on developing high-resolution digital elevation models and satellite images to identify lineaments and fault lines and evaluate tectonic activity along the eastern CKB. We conducted morphotectonic analysis on primary geomorphic indices of channel-hillslope coupling (drainage patterns, mountain front sinuosity (*Smf*), and stream-length gradient index (*SL*)) to define zones of active tectonics. These values efficiently imply the degree of tectonic activity. Our analysis reveals that most drainage patterns are dendritic, trellis, and rectangular, which indicate the patterns of joints and minor faults. The *Smf* values vary between 1 and 2.4, and the *SL* values reach the peak near the toe of the mountain and the fault segment's line. The combination of the primary geomorphic indices suggests that the eastern CKB experiences a high level of active tectonics impacted by the active MIFZ. The study highlights morphometric analysis and geomorphic indices to estimate tectonic activity and evaluate the active deformation of the landscape in the region.

Keywords

Mae Ing Fault Zone, Morphotectonic Analysis, Geomorphic Indices, Drainage Patterns, Mountain Front Sinuosity, Stream-Length Gradient Index

1. Introduction

The elevation of the Earth's surface is the product of the relationship between a tectonic process that builds topography and surficial-driven erosional processes that reduce the surface's height. Morphotectonics relies on advanced technology of age dating and remote sensing to assess the mechanisms and rate of geomorphic processes. A geomorphic marker is a displacement on a land surface that displays the differences between an initial geometry and a presently offset feature (Burbank & Anderson, 2011). However, the preservation of geomorphic markers is poor when they are older and exposed to extreme tectonic and climatic conditions. Instead, fluvial networks and hillslopes have been used as geomorphic markers for landscape changes in active regions (Kirby et al., 2007).

Lithology, geologic structures, slope gradient and topography, and climatic regimes control drainage patterns on the surface. Moreover, the spatial change in channel morphology and drainage pattern is caused by the influences of tectonic uplift and climatic perturbations (Kirby & Whipple, 2012; Whipple & Tucker, 1999; Wobus et al., 2006). Channels steepen and become more effective geomorphic agents of channel erosion (Wobus et al., 2006). Geomorphic indices are used to quantify a change in channel morphology in active tectonic regions. The indices compare the landscape's shape and imply the degree of tectonic processes and activity, climate, rock resistance, and structural geology that controls landscape evolution (Keller & Pinter, 2002).

Landscape topography and N-S striking basins in northern Thailand result from the collision of Sibumasu-Indochina terranes (Uttamo et al., 2003) and the continental extrusion between the southeastern Asian block along the major NE-SW trending India-Eurasia collision (Hodges et al., 2001). Chiang Khong Basin (CKB), a NE-SW trending basin in Chiang Rai province, Thailand, is bounded by Mae Ing Fault Zone (MIFZ) to the east. The basin is impacted by several significant earthquakes with recurrence intervals of 1500 years. The latest slip in 5200 years ago triggered the 6.9 earthquake magnitude (Wiwegwin et al., 2018). However, a change in landscape topography across the basin needs to be detailed. Our study focuses on the fault segments along the MIFZ that are considered significant control on a landscape change of the basin. We use an integration of remote sensing techniques, terrain and GIS analyses, and field observations as a tool to characterize morphotectonic landforms and to evaluate the degree of tectonic activity and deformation along the eastern CKB.

2. Geomorphic Settings of the Study Site

CKB is a geological basin that includes the area of Thoeng, Khun Tan, and Chiang Khong districts of Chiang Rai province, Thailand. It extends from northeast to southwest with a total length of 70 km and an average width of 10 km. The occurrence of the basin mainly results from the collision between the Indian-Eurasia plates, the intrusion of the Indochina mainland, and the movement of major strike-slip faults. The geologic structure of CKB is considered a

half-graben that orients in the NE-SW direction with the west dip-direction (Uttamo et al., 2003).

CKB is bounded to the east by a series of fault segments of Pak Ing, Mae Ing, Ngam Muang, Yang Hom, Khun Tan, and Thoeng (**Figure 1(a)**). The eastern side of fault segments is a mountain range that shows geomorphic features such as offset streams, alluvial terraces, v-shaped valleys, shutter ridges, and triangular facets that can be observed on satellite images and field observations. The high topography is underlain by monolithologic substrates of Permo-Triassic volcanic rocks, including rhyolite, andesite, welded rhyolitic and andesitic tuff, and volcanic breccia (Department of Mineral Resources, 1994) (**Figure 1(b)**).

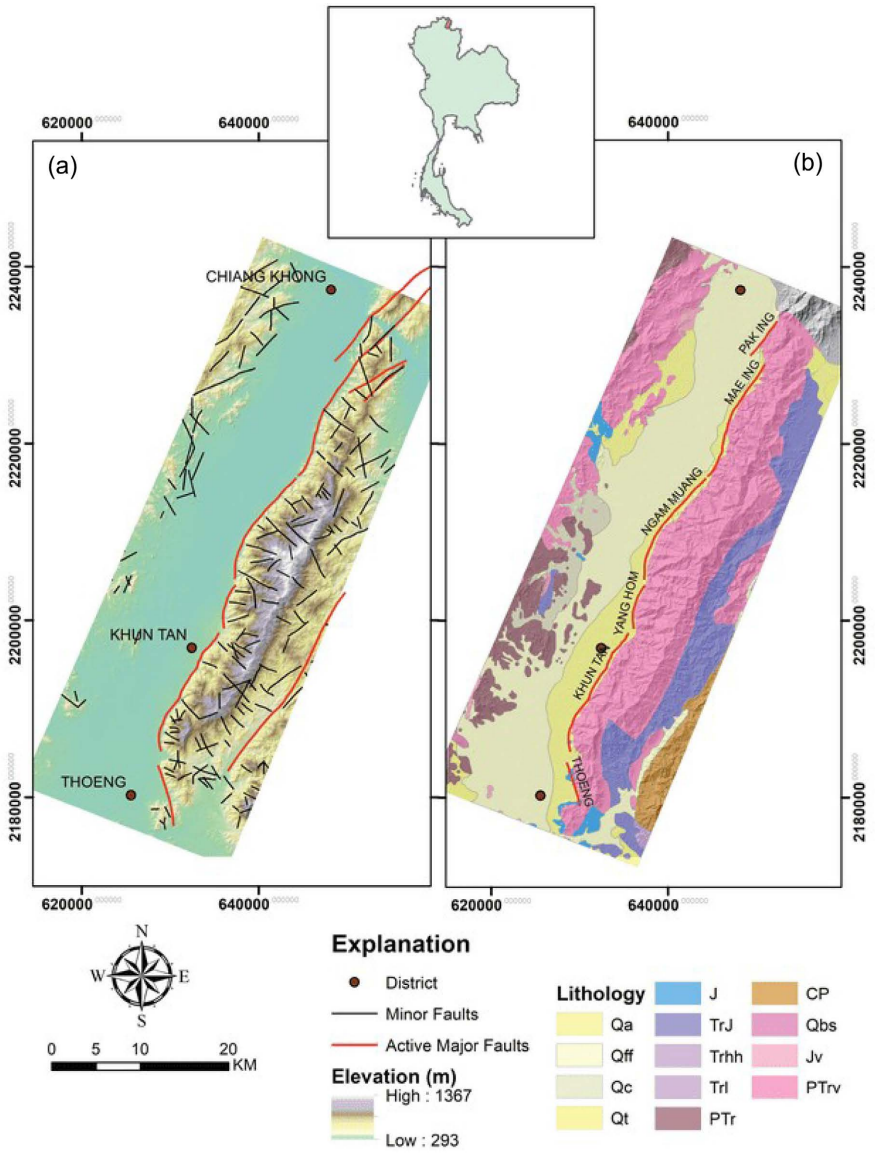

Figure 1. (a) Geographic map of the study site shows the location of fault segments (red lines) of the MIFZ in Chiang Rai, northern Thailand (inset). The name of important fault segments is labeled in (b). (b) Geologic map shows the distribution of lithology in the CKB and the MIFZ.

The Quaternary colluvial and alluvial deposits mantle the basin. The average annual accumulated rainfall obtained between 1991 and 2020 represents a minimal variation of 1700 mm across the basin (Lamphun Meteorological Department, 2020). Thus, lithologic and climatic conditions' influences are minimal relative to the role of tectonic processes in controlling the landscape topography.

3. Methodology

3.1. Channel Morphology and Fault Line Extraction

The high-resolution digital elevation model (DEM) of SRTM 1 Arc-Second Global, publicly available from ALOS satellite PALSAR, Alaska Satellite Facility, is the primary source to extract 37 low-ordered channel networks that drained from the high topography to the lower basin. We follow the step of extracting channel networks using a hydrologic toolset in ArcGIS Pro®. We characterized drainage patterns and analyzed two geomorphic indices: mountain front sinuosity (*Smf*) and stream-length gradient index (*SL*). In addition, the fault line extraction was determined from Thailand 1:50,000 scale topographic maps (L7017S) with the sheet index 5049 II, 5048 I, 5048 II, 5048 III, and 5048 IV (Methakullachat & Witchayangkoon, 2019), Landsat-8/9 satellite images on March 22, 2022, and satellite images from Google Earth Pro® using overlay analysis.

3.2. Geomorphic Indices

3.2.1. Mountain Front Sinuosity (*Smf*)

The appearance of the mountain front allows us to assess the variations in tectonic processes and erosional modification of a landform. Mountain front sinuosity (*Smf*) measures the lineament of a fault that has experienced a recent rock uplift. After discontinuous uplift, erosion predominates landscape evolution to form a sinuous mountain front, mainly where rock is less resistant. *Smf* is computed as follows (Bull & McFadden, 1977)

$$Smf = \frac{L_{mf}}{L_s} \tag{1}$$

where *Smf* is the mountain front sinuosity, L_{mf} is the length of the mountain front along the base of the mountain, and L_s is the actual distance of the mountain front (**Figure 2**). We created the sinuous lines along the toe of the mountain front with a contour interval of 20 m. We also calculated the *Smf* value at $L_s \approx 2$ km each.

3.2.2. Stream-Length Gradient Index (*SL*)

The spatial variations in the strength of active tectonics, rock resistance, and climatic conditions in the study area are determined using the stream-length gradient index (*SL*). We assess the *SL* values along longitudinal channel profiles because they are sensitive to tectonic and climatic perturbations. An anomaly on a channel profile is evidence of tectonic activity (Hack, 1973; Keller & Pinter, 2002). The index is calculated as

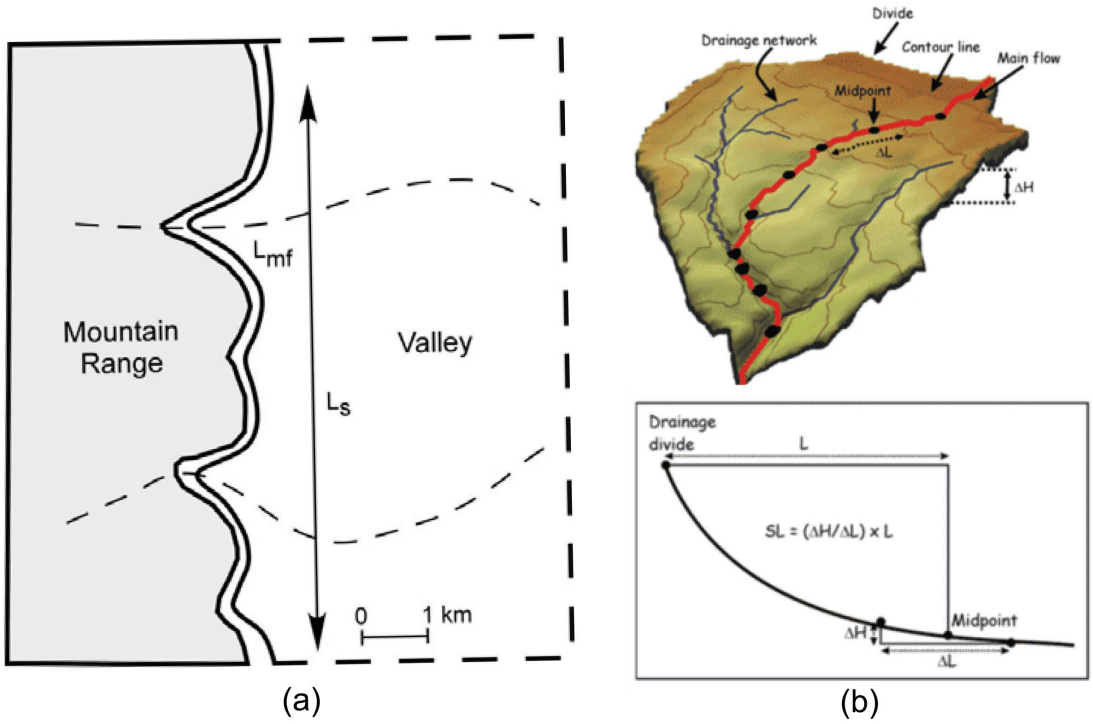

Figure 2. (a) Mountain front sinuosity or *Smf* (Keller et al., 1996). (b) (top) Stream length gradient index from the profile. (b) (bottom) The calculation of SL index for a particular reach (Font et al., 2010).

$$SL = \frac{\Delta H}{\Delta L} \times L \tag{2}$$

where SL is the stream-length gradient, $\frac{\Delta H}{\Delta L}$ is the channel slope of a particular channel reach, and L is the length from the midpoint of the reach to the topographic divide (**Figure 2**).

4. Results

4.1. Channel and Fault Line Characterization

Lower-order channels in the study site are straight and narrow. They flow from the high mountain in the east to the CKB in the west. These channels meet the meandered Mae Ing River parallel to fault segments of the MIFZ. The channels represent v-shaped valleys with some offset streams. We classified 37 channels into three types of drainage patterns: 1) 62% of total channel networks are dendritic drainage patterns where the channels flow along the slope of the terrain on smooth Permo-Triassic volcanic rocks surface, and the confluence is less than 90˚. 2) 25% of total channel networks are trellis drainage patterns where tributaries join the mainstreams at right angles due to different rock resistance. 3) The remaining 13% are rectangular drainage patterns where the mainstreams and tributaries meet at the right-angle bends. Particularly, trellis and rectangular drainage patterns can imply the presence of joints and minor faults in landscape topography (**Figure 3**).

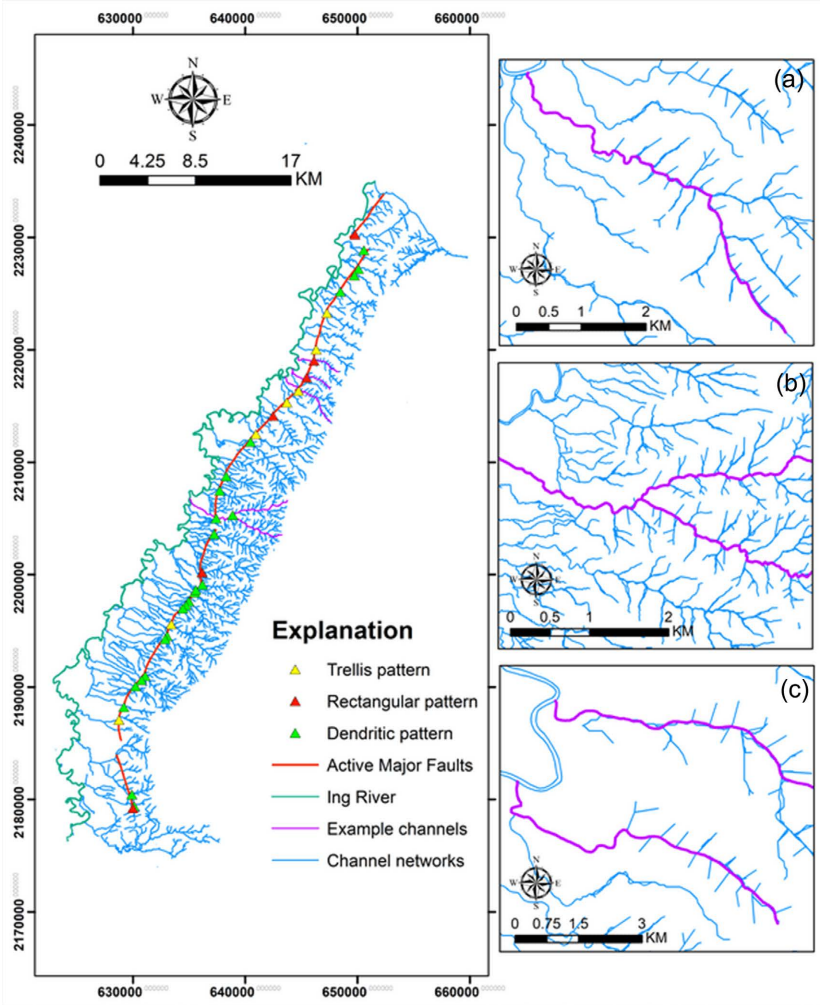

Figure 3. Map of drainage pattern along the eastern CKB and the MIFZ: (a) An example of a trellis drainage pattern in Huai Luang. (b) An example of a dendritic drainage pattern in Huai Pa Daeng Nuea and Huai Pa Daeng. (c) An example of a rectangular drainage pattern in Huai Kee Lek and Huai Kee Kwai.

4.2. Geomorphic Indices

Mountain front sinuosity (*Smf*) describes the change of the landscape from vertical and horizontal channel erosion. The *Smf* values can infer the process of rock uplift and land subsidence. Our analysis shows that the *Smf* values of 31 lineaments along the fault segments of the MIFZ range from 1.02 to 2.4. The low *Smf* values are in the central and southern zones, while the high *Smf* values are in the northern zone of the fault segments (**Figure 4**). According to *Smf* classification by Keller & Pinter (2002), the central and southern parts of the MIFZ are classified as highly active mountain ranges, while the northern part is relatively less active. Stream-length gradient index (*SL*) is calculated along 37 channels that flow from east to west. We found that the lower *SL* values are along channels in the northern and southernmost regions (channel numbers 1 - 8 and 35 - 37), while the higher *SL* values are along channels in the central zone (channel numbers 13 - 19 and 28 - 31) (**Figure 5**).

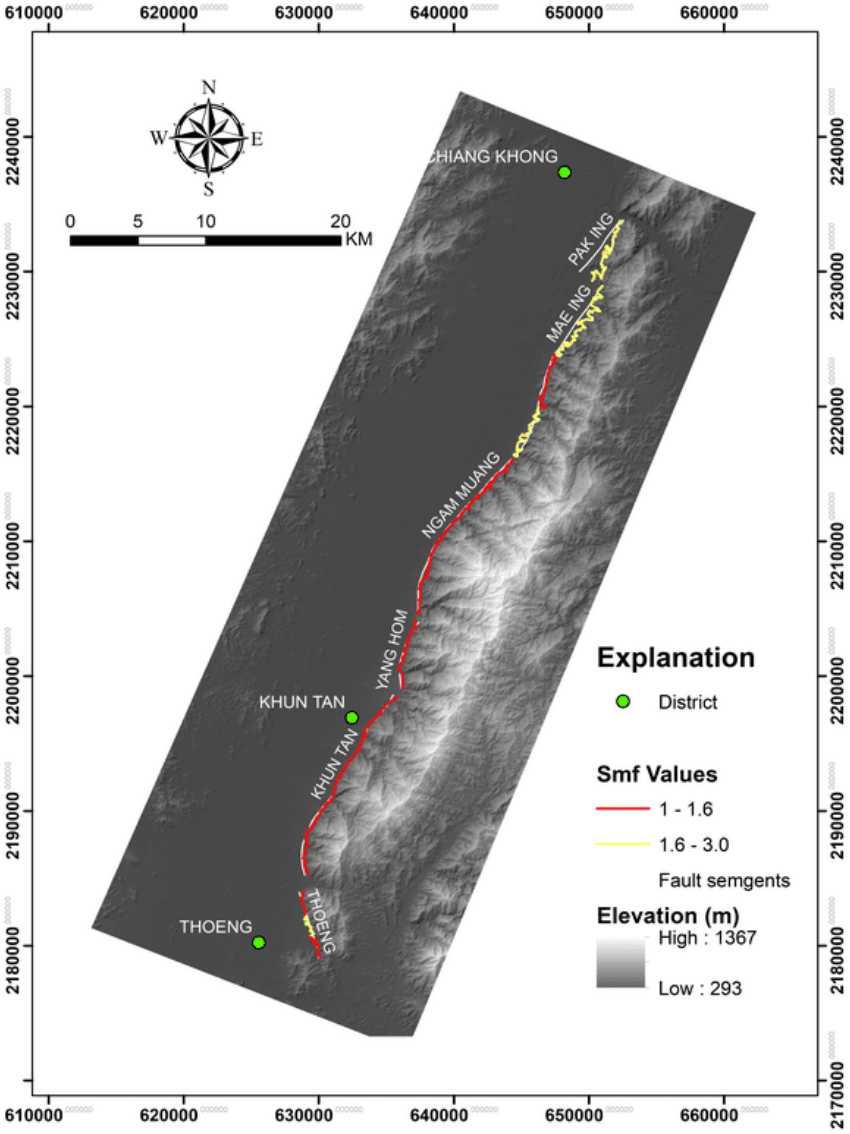

Figure 4. Map of mountain front sinuosity (*Smf*) along the eastern CKB and the MIFZ.

4.3. Geomorphic Feature Observations

We observed geomorphic features along the eastern CKB from topographic and geologic maps, Landsat 8 - 9 satellite images, Google Earth Pro®, and field observations. Topography along the fault segments depicts strike-parallel valleys, fault scarps, and triangular facets, shutter ridges, and offset streams. Strike-parallel valleys formed as near-fault landforms are found in Huai San, Huai Hok, and Huai Kaeng. Triangular facets are evidence of normal faults (**Figure 6**). Shutter ridges are found near the toe of the mountain, which has moved along a fault line and blocked the downstream flow of Huai Ruak, Huai Muang Chum, and Huai Nam Khun. Moreover, satellite images and digital elevation models show some channels that illustrate horizontal displacements, e.g., Huai Kee Lek shows an offset stream flowing toward the north and turning back to the west. Huai Yang Hom shows the southeastward offset with a turn back to the west.

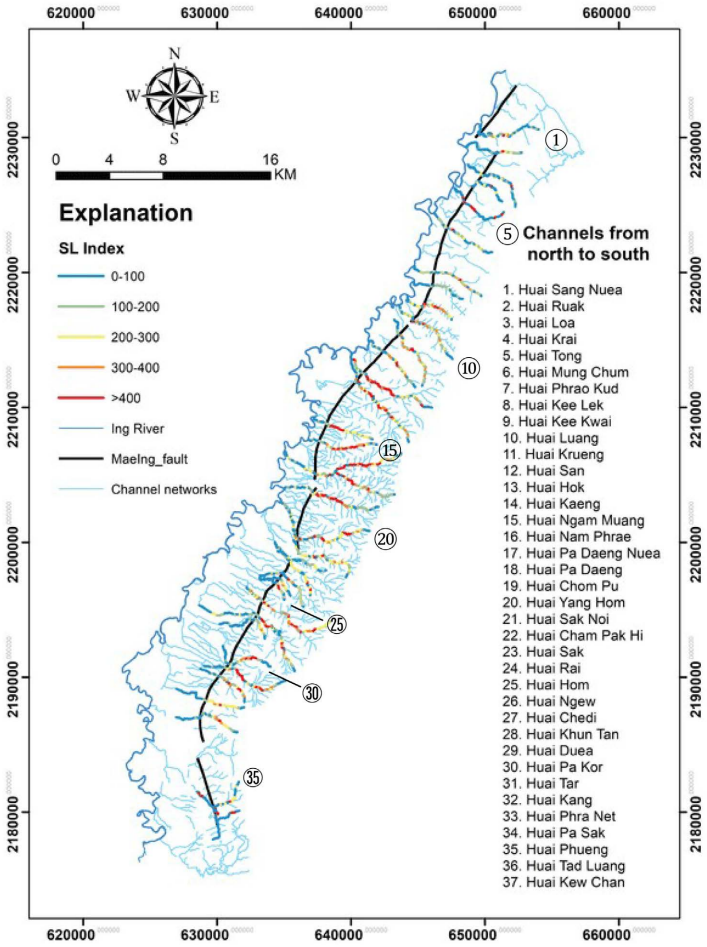

Figure 5. Map of stream-length gradient index (*SL*) along the eastern CKB.

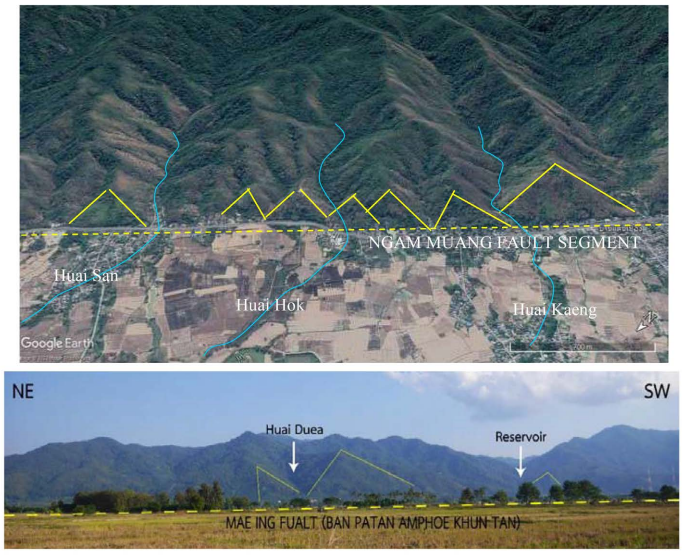

Figure 6. Top. Geomorphic features observed in satellite images from Google Earth Pro ® show a series of triangular facets (yellow triangles) and offset streams (blue lines) along the Ngam Muang fault segment of the MIFZ. Bottom: Triangular facets are shown in front of Huai Duea, Pa Tan, Khun Tan district, Chiang Rai.

5. Discussion

The collision of India-Australian to Eurasian during the Eocene or mid-Cenozoic era caused a clockwise rotation of the Eurasian plate and major dextral strike-slip faults across northern Thailand (Uttamo et al., 2003). The pull-apart CKB constraint with several oblique-slip fault segments along the MIFZ develops fault scarps and triangular facets, implying the vertical movement of the fault plane with vertical channel incision (Fenton et al., 2003). Strike-parallel valleys and major NE-SW trending offset streams on rectangular and trellis drainage patterns imply joints and minor faults on Permo-Triassic volcanic rocks.

The degree of tectonic activity is considered from the *Smf* values. The lower *Smf* values with a linear mountain front in the central and southern zones suggest the recent tectonic uplift, bedrock resistance, and less channel incision. The higher *Smf* values with a sinuous mountain front in the northern zone suggest a lower degree of tectonic and fault activity. In a homogenous rock and uniform climatic condition, channels in the central and southern zones present a peak of anomalies near the fault lines. We infer that topography in the central to southern zones of the fault segments experiences a high rock uplift and deformation. Rock uplift drives the normal-faulted terrain of the MIFZ, which also causes the spatial distribution of joints and minor faults. Fault segments are oblique-slip because of offset streams on rectangular and trellis drainage patterns. We are implementing other fault-related geomorphic indices, e.g., valley floor width-height ratio, drainage asymmetry, basin shape index, hypsometrical integral, structural geology, seismology, and geodynamics factors to analyze relative index of active tectonic (RIAT).

6. Conclusion

Landscape topography across the Chiang Khong basin is bounded by the NE-SW oblique-slip fault segments of the Mae Ing Fault Zone to the west. The high mountain in the east, underlain by Permo-Triassic volcanic rocks, presents numerous fault scarps, triangular facets, strike-parallel valleys, and shutter ridges. Channels typically flow along sloped terrains, joints, and minor faults. The lower half-graben basin in the west is a depositional area for sediment delivered from the high eastern terrain.

Morphotectonic analysis of the Chiang Khong basin relies on primary geomorphic indices of channel-hillslope coupling. Our results from the mountain front sinuosity and stream length gradient index suggest that the high degree of tectonic activity is in the central and southern parts of the fault segments. The anomaly found in longitudinal channel profiles is typically near the fault lines. In monolithologic and climatic conditions across the Mae Ing Fault Zone, the central and southern zones experience higher rock uplift, and the Mae Ing Fault Zone is still active. Our study highlights geomorphic indices as an effective tool for estimating tectonic activity and deformation in the region.

Acknowledgements

The author would like to thank several researchers, lecturers, Piyaporn Hinsaeng, and other senior students in the Department of Geological Sciences, Chiang Mai University, who supported and encouraged me to achieve the research project. Big thanks should be given to a grant from the 50th Anniversary Geology Fund that financially supported this project.

Conflicts of Interest

The author declares no conflicts of interest regarding the publication of this paper.

References

Bull, W. B., & McFadden, L. D. (1977). Tectonic Geomorphology North and South of the Garlock Fault, California. In *Geomorphology in Arid Regions Proceedings of the 8th Annual Geomorphology Symposium* (pp. 115-138). Binghamton. https://doi.org/10.4324/9780429299230-5

Burbank, D. W., & Anderson, R. S. (2011). *Tectonic Geomorphology.* Wiley-Blackwell. https://doi.org/10.1002/9781444345063

Department of Mineral Resources (1994). *Geologic Map of Changwat Chiang Rai Quadrangle Scale 1:250,000* [Online]. Geological Survey Division, Bangkok, Thailand.

Fenton, C. H., Charusiri, P., & Wood, S. H. (2003). Recent Paleoseismic Investigations in Northern and Western Thailand. *Annals of Geophysics, 46,* 957-981.

Font, M., Amorese, D., & Lagarde, J. L. (2010). DEM and GIS Analysis of the Stream Gradient Index to Evaluate Effects of Tectonics: The Normandy Intraplate Area (NW France). *Geomorphology, 119,* 172-180. https://doi.org/10.1016/j.geomorph.2010.03.017

Hack, J. T. (1973). Stream Profile Analysis and Stream-Gradient Index. *Journal of Research of the U.S. Geological Survey, 1,* 421-429.

Hodges, K. V., Hurtado, J. M., & Whipple, K. X. (2001). Southward Extrusion of Tibetan Crust and Its Effect on Himalayan Tectonics. *Tectonics, 20,* 799-809. https://doi.org/10.1029/2001TC001281

Keller, E., Pinter, N., & Green, D. (1996). *Active Tectonics, Earthquakes, Uplift, and Landscape* (1st Edition). Prentice Hall Inc.

Keller, E. A., & Pinter, N. (2002). *Active Tectonics, Earthquakes, Uplift and Landscape* (2nd Edition, p. 362). Prentice Hall. https://doi.org/10.1002/ijc.25162

Kirby, E., Johnson, C. B., Furlong, K. P., & Heimsath, A. M. (2007). Transient Channel along Bolinas Ridge, California: Evidence for Differential Rock Uplift Adjacent to the San Andreas Fault. *Journal of Geophysical Research, 112.* *https://doi.org/10.1029/2006JF000559*

Kirby, E., & Whipple, K. X. (2012). Expression of Active Tectonics in Erosional Landscapes. *Journal of Structural Geology, 44,* 54-75. https://doi.org/10.1016/j.jsg.2012.07.009

Lamphun Meteorological Department (2020). *Average Annual Accumulated Rainfall within a Period of 30 Years (1991-2020)* [Online]. Lamphun, Thailand.

Methakullachat, D., & Witchayangkoon, B. (2019). Coordinate Comparison of Google® Maps and Orthophoto Maps in Thailand. *International Transaction Journal of Engi-*

neering, Management, & Applied Sciences & Technologies, 10, 1-9.

Uttamo, W., Elders, C., & Nicholes, G. (2003). Relationships between Cenozoic Strike-Slip Faulting and Basin Opening in Northern Thailand. *Geological Society Special Publication, 210,* 89-108. https://doi.org/10.1144/GSL.SP.2003.210.01.06

Whipple, K. X., & Tucker, G. E. (1999). Dynamic of the Stream-Power River Incision Model: Implications for Height Limits of Mountain Ranges, Landscape Response Timescales, and Research Needs. *Journal of Geophysical Research, 104,* 17661-17674. https://doi.org/10.1029/1999JB900120

Wiwegwin, W., Hinsaeng, P., Junpangngern, J., & Phumsonklin, R., (2018). Characteristics of 15 Active Fault Zones in Thailand (pp. 1-233). Department of Mineral Resources, Bangkok,.

Wobus, C. W., Whipple, K. X., Kirby, E., Snyder, N., Johnson, J., Spyropolou, K., et al. (2006). Tectonics from Topography: Procedures, Promise, Pitfalls. *Tectonics, Climate, and Landscape Evolution: Geological Society of America Special Paper, 398,* 55-74.